Effectiveness of a Partially Wetted Catalyst for Bimolecular Reaction Kinetics

Gregory A. Funk,
Michael P. Harold, Ka M. Ng
Department of Chemical Engineering
University of Massachusetts
Amherst, MA 01003

A large number of studies on the effectiveness of a partially wetted catalyst particle have appeared in the literature (for example, Mills and Dudukovic, 1979; Tan and Smith, 1980; Herskowitz, 1981; Goto et al., 1981; Sakornwimon and Sylvester, 1982; Capra et al., 1982; Ring and Missen, 1986). With the exception of work by Goto et al., all these earlier studies considered only a bimolecular reaction with pseudofirst-order kinetics; i.e., first order with respect to the limiting reactant and zero order for the excess reactant. Goto et al. used pseudo-*n*th-order kinetics. Recently, Beaudry et al. (1987) and Harold and Ng (1987) demonstrated that pseudofirst-order kinetics can be misleading in that depletion of the supposedly abundant (zero-order) reactant may occur within the pellet. Also recently, Yentekakis and Vayenas (1987) suggested that bimolecular kinetics, first order with respect to each reactant, is essential for hydrodesulfurization processes.

Since zero-order kinetics in actuality loses its physical meaning when the zero-order reactant is no longer in excess and other kinetic expressions are more appropriate for some commercial processes, the objective of this work is to examine the behavior of a single reaction that is first order with respect to both gaseous and liquid reactants. Emphasis is placed on elucidating the interplay between internal diffusion, reaction, and external mass transfer on the partially wetted surface, and to examine the impact of the interplay on catalyst effectiveness.

Model Development

A two-dimensional model is developed to describe the isothermal, irreversible reaction between a dissolved gas reactant A and a nonvolatile liquid reactant B within a partially wetted, uniformly active porous catalytic pellet. As illustrated in Figure 1, the pellet has a square cross section with each side of length S and is externally wetted about the four corners. Each of the four identical liquid films is of a uniform depth and covers an equal length in both directions from the corresponding corner. The desired wetting efficiency is obtained by adjusting this length from zero to its maximum value of $S/2$, which corresponds to complete wetting. Clearly, this fixed wetting pattern is idealized, as other flow features are present in a trickle-bed reactor (Ng and Chu, 1987). The liquid phase contains the reactants, reaction product(s), and possibly an inert solvent. A gaseous environment, with a constant partial pressure of reactant A, p_{bA}, completely surrounds the wetted pellet.

The liquid phase catalytic reaction is given by

$$A_{(g)} + \nu B_{(l)} \rightarrow \text{Products}_{(l)}$$

where g and l represent gas and liquid, respectively. The intrinsic reaction rate r is assumed to be first order with respect to A and B; i.e.,

$$r = k_r C_A C_B$$

Species A and B respectively satisfy the following dimensionless diffusion-reaction equations:

$$\frac{\partial^2 u_A}{\partial s_1^2} + \frac{\partial^2 u_A}{\partial s_2^2} = \phi^2 u_A u_B \tag{2}$$

$$\frac{\partial^2 u_B}{\partial s_1^2} + \frac{\partial^2 u_B}{\partial s_2^2} = \phi^2 \frac{m}{u_{Bf}} u_A u_B \tag{3}$$

The dimensionless variables in Eqs. 2 and 3 are defined as follows:

$$u_A = \frac{C_A}{C_{Ae}} \quad u_B = \frac{C_B}{C_{Bf}} \quad s_1 = \frac{x_1}{S/2} \quad s_2 = \frac{x_2}{S/2}$$

$$\phi = \sqrt{\frac{k_r C_{Bf}}{D_{eA}}}\left(\frac{S}{2}\right) \quad m = \frac{\nu D_{eA}}{D_{eB}} \quad u_{Bf} = \frac{C_{Bf}}{C_{Ae}} \tag{4}$$

Correspondence concerning this paper should be addressed to K. M. Ng or M. P. Harold.

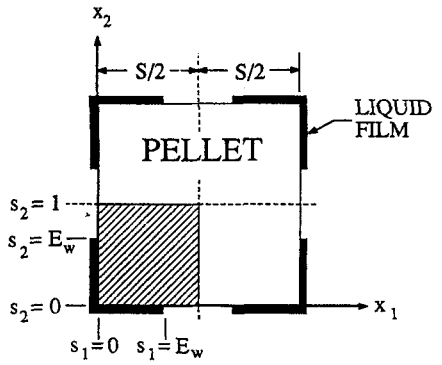

Figure 1. Square pellet wetted by four identical liquid films at the four corners.
Quadrant used for a finite-difference numerical solution is shaded

Equations 2 and 3 are solved with the following boundary conditions.

$$\frac{\partial u_A}{\partial s_i} = \frac{\partial u_B}{\partial s_i} = 0 \quad \text{at } s_i = 1 \; i = 1, 2 \tag{5}$$

$$\frac{\partial u_B}{\partial s_i} = 0 \quad \text{at } s_i = 0 \text{ (nonwetted portion) } i = 1, 2 \tag{6}$$

$$-\frac{\partial u_B}{\partial s_i} = Bi_{B,w}(1 - u_B) \quad \text{at } s_i = 0 \text{ (wetted portion) } i = 1, 2 \tag{7}$$

$$-\frac{\partial u_A}{\partial s_i} = Bi_{A,n}(1 - u_A) \quad \text{at } s_i = 0 \text{ (nonwetted portion) } i = 1, 2 \tag{8}$$

$$-\frac{\partial u_A}{\partial s_i} = Bi_{A,w}(1 - u_A) \quad \text{at } s_i = 0 \text{ (wetted portion) } i = 1, 2 \tag{9}$$

The dimensionless Biot numbers are defined as follows:

$$Bi_{B,w} = \frac{k_{lsB}}{D_{eB}}\left(\frac{S}{2}\right) \quad Bi_{A,n} = \frac{k_{gsA}}{D_{eA}}\left(\frac{S}{2}\right) \quad Bi_{A,w} = \frac{k_{lsA}}{(1+\gamma)D_{eA}}\left(\frac{S}{2}\right) \tag{10}$$

A numerical solution to the coupled, nonlinear partial differential equations, Eqs. 2 and 3, subject to the boundary conditions, Eqs. 5–9, is obtained by the method of finite differences. Detailed discussion of the numerical method will be presented elsewhere (Funk). Then, in order to examine the catalyst performance quantitatively, the catalyst effectiveness η is calculated for a wide range of conditions.

$$\eta = \frac{\int_{V_p} r(C_A, C_B)dV_p}{V_p r(C_{Ae}, C_{Bf})} \tag{11}$$

As mentioned, most previous models assumed pseudofirst-order kinetics, which we denote by PFOK. We can check the PFOK assumption using the present two-dimensional model by simplifying Eq. (1) as

$$r = (k_r C_{Bf})C_A = k_r' C_A \tag{12}$$

where k_r' is the pseudofirst-order rate constant. Then, the solution involves Eq. 2 with similar simplification and boundary conditions, Eqs. 5 (for A), 8, and 9.

Results

Concentration contours

In this section, the interaction between the chemical reaction and the various transport processes is elucidated by examining the two-dimensional reactant concentration contours. A reference set of conditions (parameter values) are selected; these are:

$$\phi = 50 \qquad Bi_{B,w} = 100.0$$
$$Bi_{A,w} = 1.0 \qquad m = 1.0$$
$$Bi_{A,n} = 100.0 \qquad u_{Bf} = 20.0$$

These conditions are intended to represent a system with the following properties:

- A highly active catalyst
- A large excess of the nonvolatile liquid reactant in the liquid film
- More effective transport of the gaseous reactant on the nonwetted portion of the catalyst

Presented in Figure 2a is the predicted two-dimensional con-

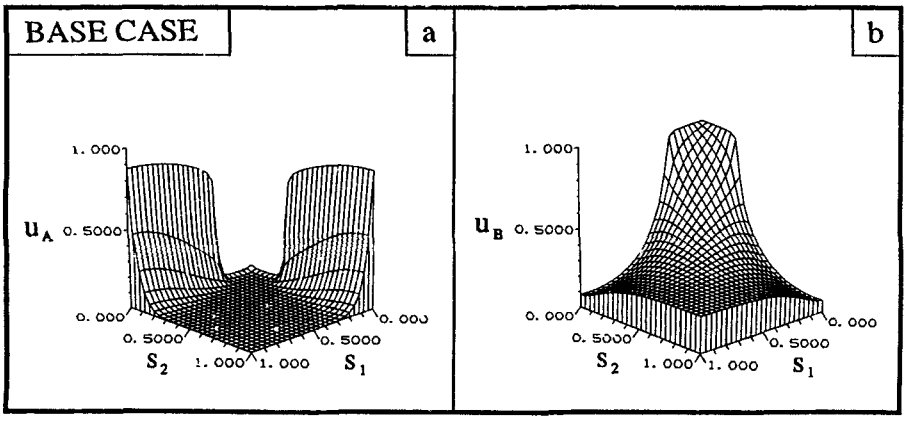

Figure 2. Species *A* and *B* concentration contours for base case.
$E_w = 0.3$; $\phi = 50$; $Bi_{A,w} = 1$; $Bi_{A,n} = 100$; $Bi_{B,w} = 100$; $m = 1$; $u_{Bf} = 20$

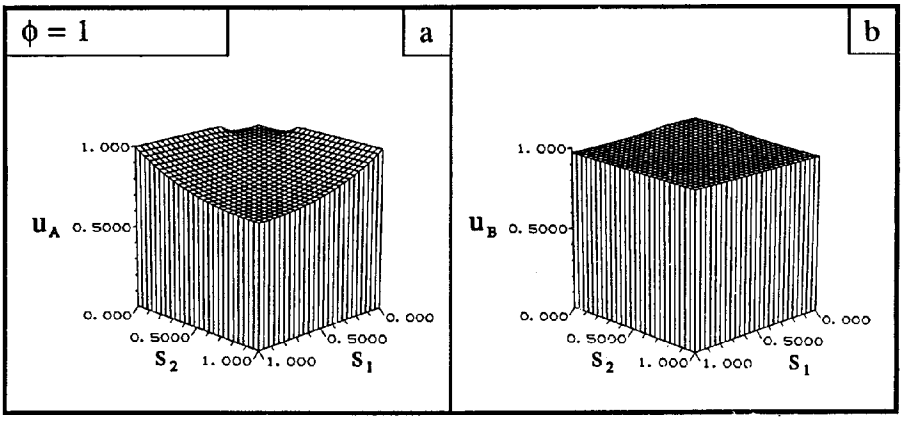

Figure 3. *A* and *B* concentration contours for $\phi = 1$.
Other parameter values as in base case

centration contour of the gaseous reactant for the reference conditions given above and a wetting efficiency E_w of 0.3. This as well as other contours are oriented in such a way that the observer is located at $s_1 = 8$, $s_2 = 8$, and $u_\alpha = 4$, viewing toward the lower left corner at (0, 0), Figure 1. Since the transport of A from the bulk gas phase is rather effective on the nonwetted surface of the pellet; i.e., from $s_1(s_2) = 0.3$ to 1.0 on $s_2(s_1) = 0$, the concentration is near its saturation value C_{Ae} near this surface. However, as one moves away from the nonwetted boundary into the interior of the pellet, the concentration of A decreases rapidly, suggesting that the system is controlled by intraparticle diffusion. Less obvious is a similar, albeit relatively small, decrease in A concentration into the pellet on the wetted surface. The external transport rate is simply much less effective than on the nonwetted part and this portion of the catalyst can also be considered to be external mass transfer controlled. In addition, notice in Figure 2a that there is a small spike at the corner (0, 0). The square cell at the corner in the grid has twice the area for the entry of A from the liquid film than does a cell further down along the straight edge of the pellet, causing a higher concentration of A at the corner.

The liquid reactant concentration contour for the same set of conditions is shown in Figure 2b. The nonvolatile B enters only through the wetted portion of the pellet; i.e., from $s_1(s_2) = 0$ to 0.3 on $s_2(s_1) = 0$. Similar to A, the concentration of B is close to its concentrations in the liquid film, u_{Bf}, but decreases toward the center of the pellet under the given conditions. Figures 2a and 2b together reveal that the overall reaction rate for the base case is limited by the slow intraparticle diffusion and external mass transport for A.

The influence of the Thiele modulus is examined in Figures 3a and 3b. The value of ϕ is decreased from 50 in Figure 2 to 1 while keeping other parameter values constant. The dimensionless intraparticle concentrations u_A and u_B are close to unity, indicating that there is a plentiful supply of both reactants. Since a decrease in ϕ corresponds to a reduction in catalytic activity, the system shifts from internal diffusion control in the base case to reaction control with a reduced Thiele modulus.

The effect of decreasing $Bi_{A,n}$ from 100 in Figure 2 to 10 is presented in Figures 4a and 4b. As expected, a reduction in the mass transfer rate of A from its base value causes a decrease in the intraparticle concentration of A, Figure 4a. Notice that u_A along the external nonwetted surface is also considerably lower than that in the base case, signifying the onset of external mass transport control of A. The intraparticle concentration of B is increased, Figure 4b, because there is less A present to consume it.

Finally, the influence of m and u_{Bf} is examined. Since these two parameters appear in the model, Eq. 3, as a ratio ($m/u_{Bf} = \upsilon D_{eA} C_{Ae}/D_{eB} C_{Bf}$, Eq. 4) only, they will be treated as a single

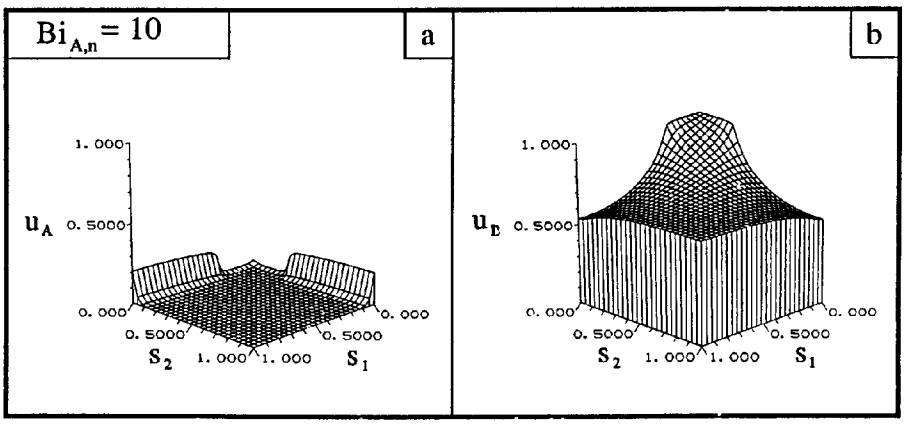

Figure 4. *A* and *B* concentration contours for $Bi_{A,n} = 10$.
Other parameter values as in base case

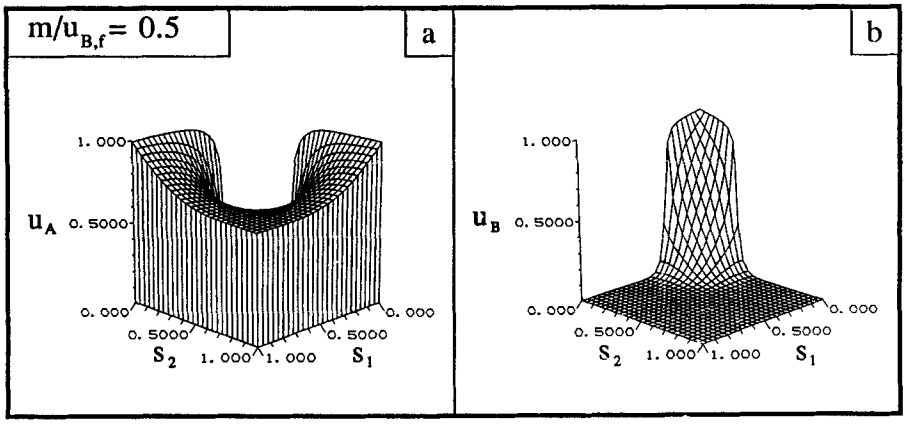

Figure 5. *A* and *B* concentration contours for $m/u_{Bf} = 0.5$.
Other parameter values as in base case

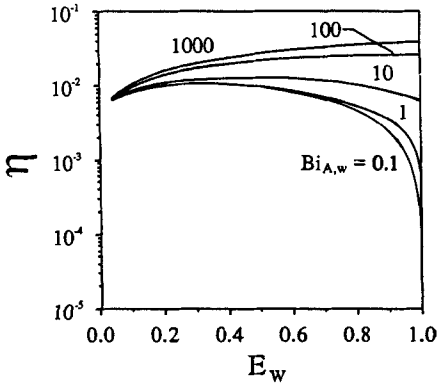

Figure 6. Dependence of effectiveness on wetting efficiency, with Biot number for *A* on the wetted part of the pellet as a parameter.
Other parameter values as in base case

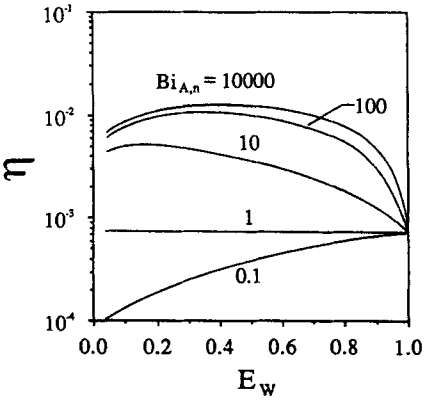

Figure 7. Dependence of effectiveness on wetting efficiency, with Biot number for *A* on the nonwetted part of the pellet as a parameter.
Other parameter values as in base case

parameter. In physical terms, large values of m/u_{Bf} result from:

1. An increase in the stoichiometric coefficient ν
2. An increasingly more effective A diffusion compared to B, or
3. An increase in the ratio of A to B concentration in the liquid film

All of these factors lead to an increase in the intraparticle concentration of A and a corresponding decline in B. Of course, one may also take the reverse argument for a decrease in m/u_{Bf}. Figures 5a and 5b correspond to an m/u_{Bf} value of 0.5, an increase from the base case value of 0.05. The intraparticle concentration of A, u_A, is close to unity over most of the pellet except near the wetted corner, where it is the limiting reactant. In the region of high A concentration, B has a concentration close to zero and is the limiting reactant. Thus, under the given conditions, there are two distinct regions within the pellet for which either A or B is the limiting reactant.

Effectiveness

In order to obtain a more comprehensive and quantitative description of reaction in a partially wetted catalyst particle, we present below effectiveness as a function of wetting efficiency for a wide variety of conditions. The following base case parameters ($Bi_{A,w} = 1$, $Bi_{A,n} = 100$, $m = 1$, $u_{Bf} = 20$) are changed one at a time so as to isolate their separate influences.

Figure 6 shows the influence of $Bi_{A,w}$. For reasons alluded to in Harold and Ng (1987), when the mass transfer of A is more effective on the nonwetted side—i.e., $Bi_{A,w} < Bi_{A,n} = 100$—$\eta$ exhibits a maximum at an intermediate wetting efficiency. When the mass transfer of A is more effective on the wetted side—i.e., $Bi_{A,w} \geq 100$—η increases monotonically with wetting efficiency. Note that all the curves merge for small values of E_w, the reason being that the reaction is limited by the supply rate of the liquid reactant at a low wetting efficiency.

The effect of $Bi_{A,n}$ is shown in Figure 7. As in the last case, Figure 6, effectiveness enhancement occurs if $Bi_{A,n} > Bi_{A,w}$ (=1 here). If $Bi_{A,n} < Bi_{A,w}$, again as in the previous case, η increases monotonically with wetting efficiency. Note that all the curves meet at $E_w = 1$ since a fully wetted pellet has no dependence on $Bi_{A,n}$. When $Bi_{A,n} = Bi_{A,w} = 1$, η is independent of wetting efficiency. This is in sharp contrast to the case with $Bi_{A,n} = Bi_{A,w} = 100$, where η increases with wetting efficiency, Figure 6. This difference is caused by the fact that with a high Biot number for

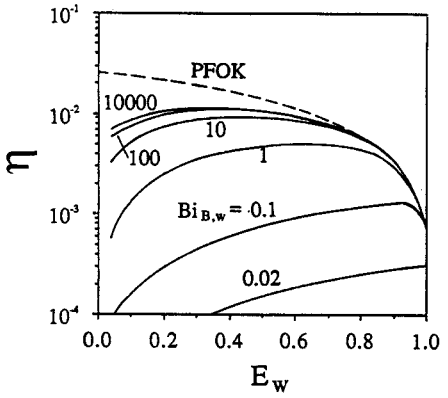

Figure 8. Dependence of effectiveness on wetting efficiency, with the Biot number for *B* on the wetted part of the pellet as a parameter.
Other parameter values as in base case

species A there is an ample supply of gaseous reactant, and a higher wetting efficiency provides more liquid reactant for reaction. At a low Biot number for species A the overall rate is limited by the external supply rate of the gaseous reactant. With an oversupply of liquid reactant, η is insensitive to wetting efficiency.

Figure 8 shows that the effectiveness increases with an increase in the Biot number for B. This is of course a result of an improved mass transfer rate of B. Although it is not clear from the figure, the curves for $Bi_{B,w} \geq 1$ end up close to each other but do not intersect at $E_w = 1$. With $Bi_{A,w} = 1$, the overall reaction rate is controlled by the external supply of A for a pellet fully covered with liquid and η is insensitive to $Bi_{B,w}$ under the complete wetting conditions. For sufficiently small $Bi_{B,w}$ (e.g., $Bi_{B,w} = 0.02$,) the effectiveness does not exhibit a maximum and its value at $E_w = 1$ decreases considerably with $Bi_{B,w}$ as the reaction becomes external B mass transfer controlled.

Finally, the influence of m/u_{Bf} is presented in Figure 9. Effectiveness is improved with a decrease in m/u_{Bf}, which corresponds to an increase in the supply of B. As in Figure 8, these curves are close to each other at $E_w = 1$ for the same reason stated earlier.

The dashed curves in Figures 8 and 9 are the model prediction

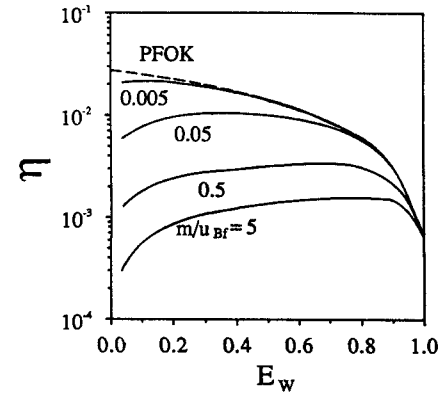

Figure 9. Dependence of effectiveness on wetting efficiency with ratio m/u_{Bf} as a parameter.
Other parameter values as in base case

for the base case except that the pseudofirst-order kinetics assumption is invoked, Eq. 12. Note that since the solution has no dependence on the zero-order reactant, $Bi_{B,w}$, m, and u_{Bf} have no influence on the PFOK solution. As can be seen in these figures, PFOK provides a good approximation to the actual solution if the wetting efficiency is sufficiently high or if there is an ample supply of B. However, the PFOK solution invariably fails at sufficiently low wetting efficiency for lack of liquid reactant.

Acknowledgment

This work was performed under National Science Foundation Grant No. CBT-8700554.

Notation

A = gaseous reactant
B = liquid reactant
Bi = Biot numbers, Eq. 10
C = liquid phase concentration
C_{Ae} = concentration of A in equilibrium with its bulk partial pressure
D_e = effective diffusivity
E_w = wetting efficiency
k = mass transfer coefficient
k_r = rate constant
k'_r = pseudofirst-order rate constant
m = parameter, Eq. 4
P_{bA} = bulk partial pressure of A
r = reaction rate
S = width of square catalyst pellet
s_1, s_2 = dimensionless coordinates, Figure 1
u = dimensionless concentration
V_p = volume of catalyst
x_1, x_2 = coordinates, Figure 1

Greek letters

α = dummy index for either A or B
γ = ratio of k_{lsA} to k_{glA}
η = effectiveness
ν = stoichiometric coefficient
ϕ = Thiele modulus

Subscripts

e = equilibrium
f = film
g = gas
i = dummy index
l = liquid
n = nonwetted
s = solid
w = wetted

Literature Cited

Beaudry, E., M. P. Dudukovic, and P. L. Mills, "Trickle-Bed Reactors: Liquid Diffusional Effects in a Gas-Limited Reaction," *AIChE J.*, **33**, 1435 (1987).

Capra, V., S. Sicardi, and A. Gianetto, "Effect of Liquid Wetting on Catalyst Effectiveness in Trickle-Bed Reactors," *Can. J. Chem. Eng.*, **60**, 283 (1982).

Funk, G. A., Ph.D. Diss. in progress.

Goto, S., A. Lakota, and J. Levec, "Effectiveness Factors of *n*th-Order Kinetics in Trickle-Bed Reactors," *Chem. Eng. Sci.*, **36**, 157 (1981).

Harold, M. P., and K. M. Ng, "Effectiveness Enhancement and Reactant Depletion in a Partially Wetted Catalyst," *AIChE J.*, **33**, 1448 (1987).

Herskowitz, M., "Wetting Efficiency in Trickle-Bed Reactors. The Overall Effectiveness Factor of Partially Wetted Catalyst Particles," *Chem. Eng. Sci.*, **36**, 1665 (1981).

Mills, P. L., and M. P. Dudukovic, "A Dual-Series Solution for the Effectiveness Factor of Partially Wetted Catalysts in Trickle-Bed Reactors," *Ind. Eng. Chem. Fundam.*, **18**, 139 (1979).

Ng, K. M., and C. F. Chu, "Trickle-Bed Reactors," *Chem. Eng. Prog.*, **38**(11), 55 (1987).

Ring, Z. E., and R. W. Missen, "Trickle-Bed Reactors: Effect of Wetting Geometry on Overall Effectiveness Factor," *Can. J. Chem. Eng.*, **64**, 117 (1986).

Sakornwimon, W., and N. D. Sylvester, "Effectiveness Factors for Partially Wetted Catalysts in Trickle-Bed Reactors," *Ind. Eng. Chem. Process Des. Dev.*, **21**, 16 (1982).

Tan, C. S., and J. M. Smith, "Catalyst Particle Effectiveness with Unsymmetrical Boundary Conditions," *Chem. Eng. Sci.*, **35**, 1601 (1980).

Yentekakis, I. V., and C. G. Vayenas, "Effectiveness Factors for Reactions Between Volatile and Nonvolatile Components in Partially Wetted Catalysts," *Chem. Eng. Sci.*, **42**, 1323 (1987).

Manuscript received July 28, 1987, and revision received Jan. 4, 1988.